



Photonic Bandgap Properties of One-Dimensional Bilayer Periodic Structure Composed of Silicon Dioxide and Gallium Phosphide Material Layers

Arafa H. Aly¹ · Bhuvneshwer Suthar^{2,3} · Azath Mubarakali^{1,3} ·
Suhad Ali Osman Abdallah⁴ · S. K. Awasthi⁵ · Emadelden Fouad⁶ · M. I. Fathy¹

Received: 9 November 2023 / Revised: 11 January 2024 / Accepted: 29 January 2024
© The Author(s), under exclusive licence to Springer Science+Business Media, LLC, part of Springer Nature
2024

Abstract

In the present work, we have investigated the optical properties of various one-dimensional photonic crystals composed of alternate material layers of silicon dioxide (SiO₂) and gallium phosphide (GaP). The choice of GaP material is due to its larger bandgap property with better thermal stability. It belongs to the category of an indirect bandgap semiconductor is commonly used in light-emitting diodes. The optical characteristics of various one-dimensional PCs consisting of different period number N have been investigated by using the transfer matrix approach. The transmittance and absorption characteristics of all structures have been examined. The present study also includes characteristics of the reflectance phase and relative percentage reflectance of all photonic structures. The dependence of the transmission characteristics of all structures on the thickness of SiO₂ and GaP material layers as well as on the incident angle corresponding to TE wave only have been also discussed in this work. Unlike two-dimensional and three-dimensional PCs the fabrication of one-dimensional photonic structures is easier. Any of the suitable thin film deposition techniques available at present can be used for the realization of such structures.

Keywords Photonic crystals · Gallium phosphide · Silicone dioxide · Transfer matrix

1 Introduction

Optical materials of size nano or micro level are named as photonic crystals (PCs) made up of periodically arranged dielectric. They have special ability of restricting light of specific frequency or wavelength depending upon the polarization condition

Extended author information available on the last page of the article

of the light passing through them [1, 2]. The restricted frequency or wavelength regime of light is defined as photonic bandgap (PBG), which helps in determining the characteristics properties of PCs. The periodic arrangement of the dielectrics in space is used to categorize them as a one-dimensional (1-D), two-dimensional (2-D) & three-dimensional (3-D) PCs [1–5]. The fraction of incoming light incident on the PC is reflected by the interface between the periodically arranged alternating layers of the structure. The superposition between the incident and reflected waves is responsible for the formation of standing waves inside photonic structures. Any modification in the sequencing of the nanostructured composite layers of the structure yields the change in the optical response of the structure [6–9]. Besides this they also have tremendous ability of modulating the propagation of light passing through them. This unprecedented control over the propagating light makes them suitable to be used in numerous potential applications such as designing of optical filters, photonic switches, dense wavelength division multiplexers, optical sensors and so on [10–17]. The biosensors composed of 2-D square photonic lattice for detection of concentration of Glucose and Creatinine in blood has been studied by Rafiee [18]. Rafiee et al. suggested a photonic power splitter suitable for integrated photonic circuits can be used to drive multiple optical devices [19]. Some other useful applications of 2-D PCs as a ring shaped demultiplexer and optical add drop filter have been realized by Rafiee et al. in references [20] and [21] respectively.

The present technological developments of material science opens new gateway of designing conventional and unconventional photonic devices of extraordinary caliber due to the availability of various novel materials. Gallium phosphide (GaP) is amongst such materials which has emerged as a significant player in the field of photonic engineering since 1960s. Despite of having an indirect gap, GaP is used prominently in the variety of light-emitting products, such as green LEDs [22]. Its larger band gap characteristics with better thermal stability is amongst the most suitable feature of GaP which encourage the researchers to use this material extensively in designing of various optoelectronic devices of diversified nature [23]. The nano-photonic devices consisting of defective GaP material are extensively used as a fluorescent and nitrogen vacancy center emitters [24, 25]. These defective structures are very useful for illustrating their application as a spectrometer [26], second harmonic production [27, 28] and some of nonlinear optical phenomenon like sum-frequency generation (SGF) [29]. Actually persistent behavior of GaP due to its non-centrosymmetric crystalline nature is responsible for achieving accurate measurement of second-order susceptibility in visible and infrared nonlinear crystals [30], micro hardness value of 9450 N/mm², Debye temperature of 446 K with thermal expansion coefficient of $5.3 \times 10^{-6} \text{ K}^{-1}$ at room temperature [23]. The bandgap of GaP is 2.24 eV which is large and responsible for reducing the thermal and other losses associated with the photonic devices whose operating wavelength is more than 1100 nm in the infrared wavelength regime. The presence of GaP material as a constituent material in the design of photonic devices allows them to function in the visible range of electromagnetic spectrum. Moreover, the significantly higher refractive index value of 3.05 at wavelength 1600 nm, makes GaP as a promising candidate to confine the optical photon in low refractive region regions [26–30].

In the present study, silicon dioxide layers are alternated with gallium phosphide layers to form the proposed structures of different period numbers (N). The optical characteristics of proposed 1-D photonic structures are investigated by using transfer matrix approach. The dependence of the optical characteristics as a function of thicknesses of layers SiO_2 and GaP, period number of the structure and incident angle corresponding to TE-polarized light have also included into the present work. This work claims the feasibility of designing a 1D photonic structure composed of SiO_2 and GaP material layers in the infrared region of electromagnetic spectrum. As per our best of knowledge, numerical investigations of this kind of photonic structures containing semiconductors have rarely explored. In addition, the present work also includes the comparison analysis pertaining to the structures composed of different semiconductors.

2 Structure and Method

This section of the manuscript deals with structural details of the proposed 1-D PC design composed of isotropic and homogeneous layers of materials SiO_2 and gallium phosphide GaP as shown in Fig. 1. The architecture of the proposed 1-D photonic design is defined as $(\text{SiO}_2/\text{GaP})^N$, where N is the period number of the structure. The thicknesses and refractive indices of alternated layers of material SiO_2 and GaP are denoted as d_1 & d_2 and n_1 & n_2 respectively. The alternate layers of materials SiO_2 and GaP of the structure are periodically arranged along z -direction whereas both the layers are homogeneous along x - and y -directions. To make our work simple the plan wave propagation along z -direction has been considered.

Next efforts have been given to introduce the theoretical formulation of the proposed work. All the simulations of the proposed work have been done by using MATLAB software as a computation tool to extract the reflectance and transmittance properties of the proposed designs. The transfer matrix method (TMM) which is one of the precise, simple and suitable approach for simulating results of finite sized 1-D photonic structures has been adopted for getting

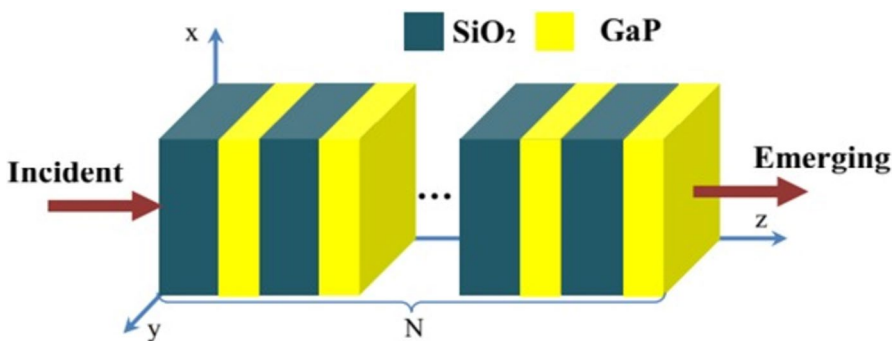


Fig. 1 A schematic diagram of 1-D PC composed of SiO_2 and GaP material layers shown in dark green and yellow colours respectively. Periodicity of the structure is along z -direction

MATLAB results. It is amongst the most intriguing techniques for analyzing the interaction of an electromagnetic waves with the interfaces of the periodic multilayer structure. This technique utilizes the continuity condition for establishing the relations between the tangential and normal components of both electric and magnetic fields at the interface separating the two material layers of the structure. The transfer matrix of any ζ^{th} layer of the design can be written as [32, 33]

$$T_{\zeta} = \begin{bmatrix} \cos\xi_{\zeta} & \frac{i}{\kappa_{\zeta}} \sin\xi_{\zeta} \\ -i\kappa_{\zeta} \sin\xi_{\zeta} & \cos\xi_{\zeta} \end{bmatrix} \tag{1}$$

where, $\xi_{\zeta} = \frac{2\pi n_{\zeta} d_{\zeta} \cos\theta_{\zeta}}{\lambda}$ is the phase angle associated with ζ^{th} layer of the structure ($\zeta = 1, 2$). The symbols n_{ζ} , d_{ζ} and θ_{ζ} are used to represent refractive index, thickness and ray angle inside ζ^{th} layer of the structure. The symbol λ is used for free space wavelength. For TE polarized wave $\kappa_{\zeta} = n_{\zeta} \cos\theta_{\zeta}$. The resultant transfer matrix of entire 1-D photonic structure can be obtained by multiplying transfer matrices of each layer of the structure one by one as

$$T = (T_1 \cdot T_2 \cdot \dots)^N \tag{2}$$

Here notations T_1, T_2, \dots are being used to represent the transfer matrix of first, second, ... layer respectively of the structure. The symbol N is representing period number of the structure. The transmittance (\mathcal{J}), and reflectance (R) of the entire structure can be obtained from the following relations as

$$\mathcal{J} = \left| \frac{2\kappa_i}{(X_{11} + \kappa_s X_{12})\kappa_i + (X_{21} + \kappa_s X_{22})} \right|^2 \tag{3}$$

and

$$R = \left| \frac{(X_{11} + \kappa_s X_{12})\kappa_i - (X_{21} + \kappa_s X_{22})}{(X_{11} + \kappa_s X_{12})\kappa_i + (X_{21} + \kappa_s X_{22})} \right|^2 = |R|e^{i\phi} \tag{4}$$

Here X_{11}, X_{12}, X_{21} and X_{22} are elements of the transfer matrix representing the entire structure [34].

The notations κ_i and κ_s used in Eqs. (3) and (4) are corresponding to incident and exit media respectively. The air has been considered as media both sides of the structure. The absorptance (A) of the 1D PC design can be obtained by using the following relation as

$$A = 1 - R - \mathcal{J} \tag{5}$$

The reflectance phase ϕ associated with the reflected wave from the proposed structure can be according to Eq. (6) as [35–38]

$$\phi = \arg(R) \pm m\pi \tag{6}$$

The relative percentage reflectance (\mathcal{R}) of the proposed structure has been defined as

$$\mathcal{R} = \frac{R}{(R + \mathcal{T})} \quad (7)$$

where, $m=0, 1, 2, 3, \dots$

3 Results and Discussions

First, we have initially chosen the thicknesses d_1 and d_2 of material layers of SiO_2 and GaP of the proposed 1-D photonic structure as 87 nm and 35 nm respectively. The period number of the structure has been fixed to 4. The transmittance of the various photonic structures of $d_1=87$ nm and $d_2=35$ nm, 55 nm, 75 nm, and 95 nm have been plotted by using Eqs. (1) to (7). The transmittance of the all photonic structures with $d_2=35$ nm, 55 nm, 75 nm and 95 nm are shown in Fig. 2.

The proposed work deals with the wider range of an electromagnetic spectrum extending from ultraviolet to infrared region ranging from 300 to 1800 nm. It has been observed that as thickness d_2 increases from 35 to 95 nm in steps of 20 nm, the higher edge of respective photonic bandgaps (PBGs) start shifting towards higher wavelength side as evident in Fig. 2. Moreover, the change in thickness of d_2 layer from 35 to 55 nm results the shift in the position of PBG from ultraviolet to visible region of electromagnetic spectrum. Further increase in the thickness d_2 from 55 to

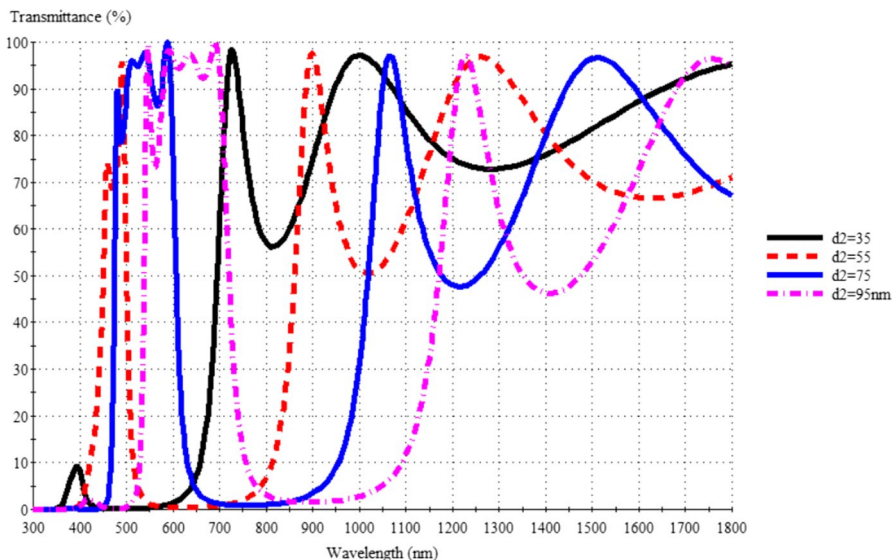


Fig. 2 Transmittance of proposed 1-D photonic structure $(\text{SiO}_2/\text{GaP})^4$ corresponding to $d_1=87$ nm and $d_2=35$ nm, 55 nm, 75 nm, and 95 nm at normal incidence. The solid black, red dotted, blue solid and pink dashed dotted lines are corresponding to $d_2=35$ nm, 55 nm, 75 nm and 95 nm respectively (Color figure online)

75 nm results the shifting of PBG towards infrared region in such a way that almost 50% of PBG containing lower band edge remains in the visible region whereas as 50% of the PBG containing higher edge of PBG falls into infrared region of electromagnetic spectrum. As the thickness d_2 reaches to 95 nm the entire PBG shifted into the infrared region of electromagnetic spectrum.

Next, attention has been given to examine the effect of change in the incident angle corresponding to TE wave only, on the transmittance of the 1-D photonic structures of period number $N=1, 2, 4, 6, 8, 10$ and 12 . For this purpose, the incident angle has been varied from 0° to 90° in steps of 10° . The thicknesses of SiO_2 and GaP material layers have been fixed to $d_1=87$ nm and $d_2=55$ nm respectively. The transmittance spectra of structures of period number $N=1, 2, 4, 6, 8, 10$ and 12 corresponding have been plotted in Fig. 3. It shows that the transmittance of 1-D photonic structure with $N=1$ shown by dashed red line curve remain nearly 55% corresponding to change in the incident angle from 0° to 80° . Further increase in the incident angle from 80° suddenly reduces the transmittance which reaches to zero at 90° . Almost similar behavior has been noticed for the structures with $N=2$ and $N=3$. Though the transmittance of structure with $N=2$ varies between maximum of 30% to minimum of 26% corresponding to change in angles from 0° to 80° which becomes zero at $\theta=90^\circ$. The structure with $N=4$ shows the sudden and significant fall in transmittance which varies between 17% at $\theta=0^\circ$ to 10% at $\theta=80^\circ$. Transmittance gradually decreases and becomes 0 at $\theta=90^\circ$. Further increase in the

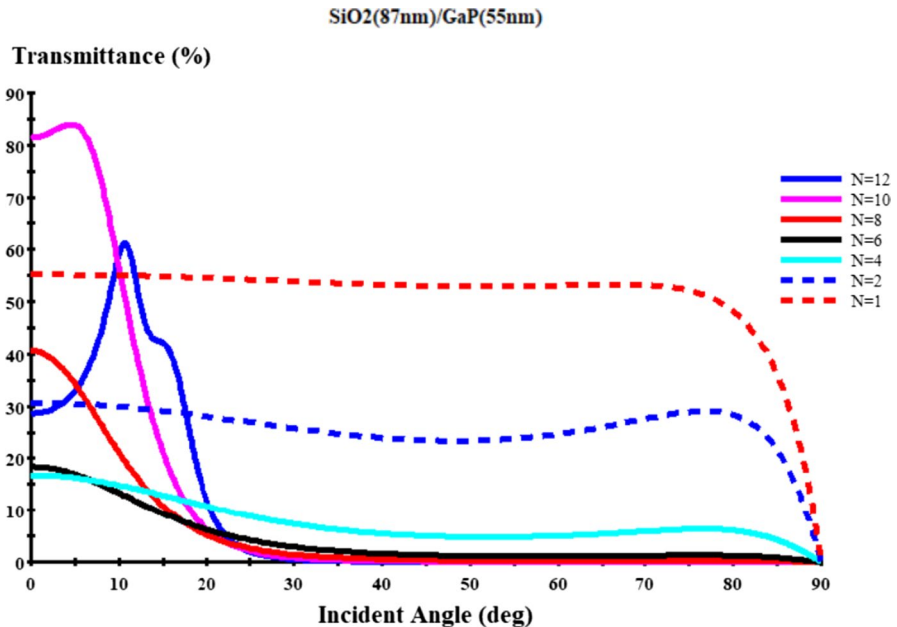


Fig. 3 Angle dependent transmittance of proposed 1-D photonic structures $(\text{SiO}_2/\text{GaP})^N$ of SiO_2 layer thickness $d_1=87$ nm and GaP layer of thickness $d_2=55$ nm corresponding to different period numbers $N=1, 2, 4, 6, 8, 10$ and 12 . The angular transmittance of all structures is calculated only for TE polarized wave

period number from $N=4$ possess significant down fall in the transmittance between the angle $\theta=27^\circ$ to $\theta=90^\circ$ due the increase in the number of interfaces between the layers of the structure. This improvement results the enhancement in the reflection range of the wavelength resulting PBG. The structure corresponding to $N=12$ shows PBG of sharp edges which is terminated at $\theta=90^\circ$. This observation explores the possibility of using proposed structure of $N=12$ as a broad band angular reflector [39].

Next, we turn our attention to examine (a) reflection phase and the relative percentage reflectance as defined by Eqs. (6) and (7) respectively, (b) transmittance and the relative percentage reflectance as defined by Eqs. (3) and (7) respectively along with (c) absorptance and the relative percentage reflectance as defined by Eqs. (5) and (7) respectively, of the 1-D PC design of period number $N=1$ composed of SiO_2 and GaP layers of thickness 55 nm and 87 nm respectively with respect to free space wavelength with the help of plots shown in Figs. 4a–c respectively under normal incidence.

As evident from Fig. 4a the polarity of the reflectance phase shift changes at the edges of PBGs of 1-D PC structure. This behavior is similar to the behavior reported in Ref. [38]. The sudden change in the reflection phase (ϕ) is noticed at the lower and higher band edges of both the PBGs as shown in Fig. 4a. The relative percentage reflectance \mathcal{R} shows a sharp dip at the lower edge of second PBG. The

SiO₂(87nm)/GaP(55nm), N=1, Normal

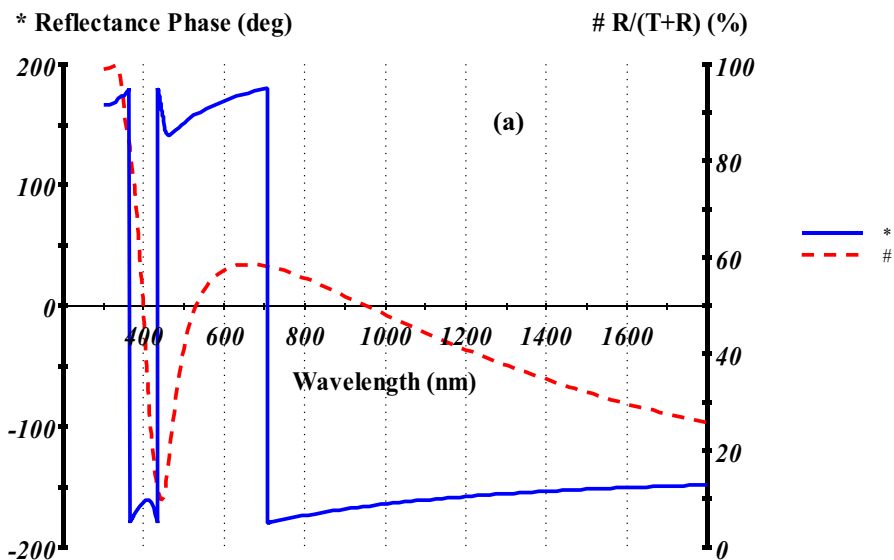


Fig. 4 Dependence of **a** reflection phase and the relative percentage reflectance, **b** transmittance and the relative percentage reflectance and **c** absorptance and the relative percentage reflectance on the free space wavelength of 1D photonic crystal ($N=1$) of alternating layers of materials SiO_2 and GaP of thicknesses 55 nm and 87 nm respectively under normal incidence

SiO₂(87nm)/GaP(55nm), N=1, normal

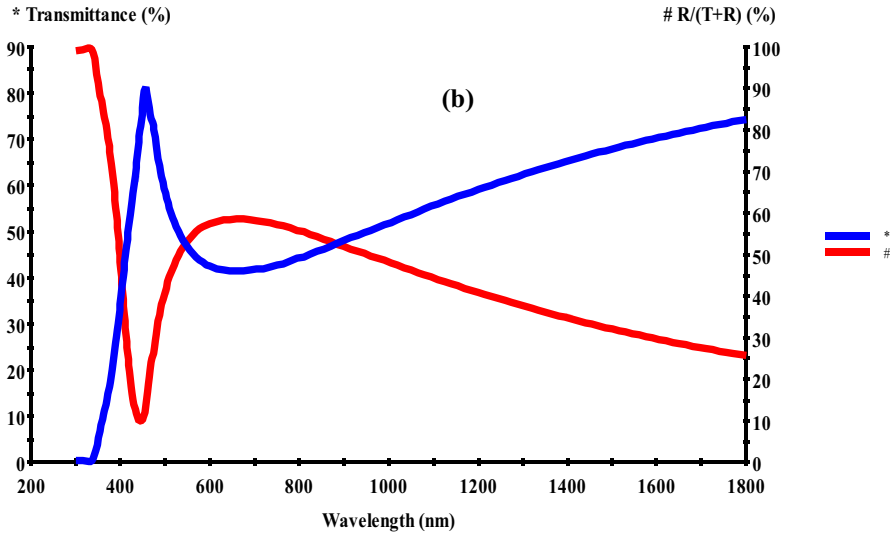


Fig. 4 (continued)

SiO₂(87nm)/GaP(55nm), N=1, Normal incidence

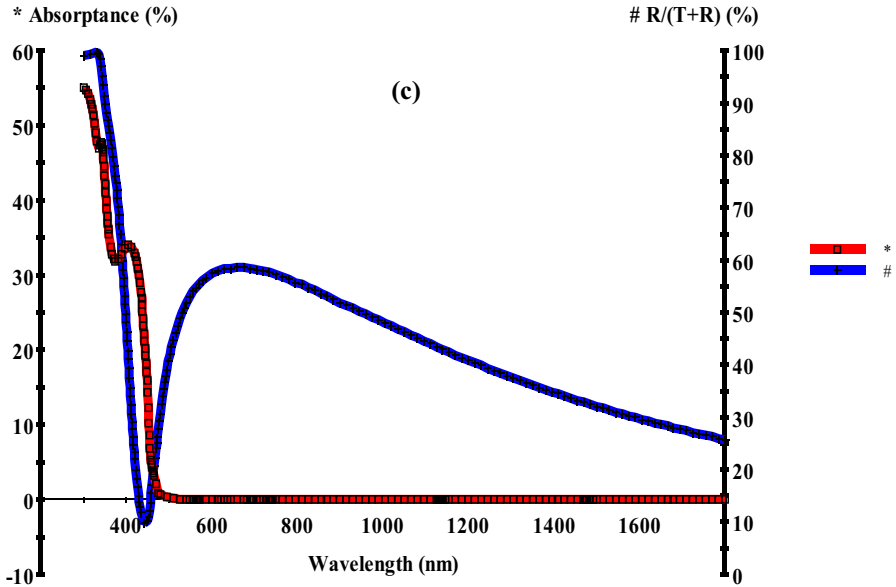


Fig. 4 (continued)

dip reaches to its maximum value around 600 nm inside second PBG which reaches to its minimum value at 1800 nm.

Next, we have studied the how \mathcal{J} and \mathcal{R} of the structure changes with the free space wavelength. These various are being plotted in Fig. 4b. It shows that the nature of change in \mathcal{J} and \mathcal{R} dependent upon free space wavelength is opposite to each other. The value of \mathcal{J} reaches to minimum whereas \mathcal{R} reaches to maximum at the free space wavelength around 450 nm. This property can be utilized for designing of an optical switch as well as antireflection coatings.

Finally, an attention has been paid to examine the absorption characteristics of the structure depending upon the wavelength in contrast to the wavelength dependent properties of \mathcal{R} . These variations are being shown in Fig. 4c. Figure 4c shows that the absorptance of the structure reaches to zero from 490 to 1800 nm i.e. our structure possesses zero absorptance in the entire infrared region as well as most of the part of visible part of an electromagnetic spectrum. The relative percentage reflectance starts to reduce and becomes minimum at the lower band edge as free space wavelength increases from ultraviolet to visible part of the spectrum. Further increase in the wavelength results the increase in value of \mathcal{R} which is reached to maximum value of 60% around 600 nm. The value of \mathcal{R} can be further reduced to 28% at 1800 nm. This variation is due to the significant increase in the value of an extinction coefficient of material in ultra violet to lower part of visible spectrum.

Next, the effect of incident angle on the wavelength dependent transmittance characteristics of 1-D photonic structure composed of alternating material layers of SiO_2 and GaP of period number $N=1$ have been studied. This purpose has been fulfilled by plotting a 3-D plot showing the effect of change in the incident angle on the wavelength dependent transmittance characteristics of 1-D photonic structure as shown in Fig. 5. It can be clearly seen that under normal incidence the transmittance of the structure shows sharp single peak which becomes wider with an increase in the incident angle corresponding to TE polarized wave. The transmittance characteristics of the structure can be easily explained with the help of interference phenomenon between rays reflected from the various interfaces between any two adjacent layers of the structure.

Further we have focused our attention to study the effect of changing thickness d_1 of material layer SiO_2 of the photonic structure $(\text{SiO}_2/\text{GaP})^N$ with $N=1$ under normal incidence. For this study Fig. 6 has been plotted. It contains five transmittance plots shown in black solid line, blue solid line, red solid line, pink solid line and blue dashed line corresponding to thickness 20 nm, 40 nm, 60 nm, 80 nm and 100 nm of SiO_2 material layers of structures with $d_2=95$ nm, $N=1$ and $\theta=0^\circ$. It has been observed that the increase in the thickness of SiO_2 layer the transmittance of the respective structure improves and becomes maximum at fixed value of wavelength corresponding to the structure with $d_1=100$ nm. Additionally, PBG corresponding to all structures remains almost same.

Finally, we have examined the effect of increasing the number of unit cells (N) on the transmittance spectra of the structure $(\text{SiO}_2/\text{GaP})^N$ with $d_1=87$ nm, $d_2=55$ nm, $N=1$ and $\theta=25^\circ$ corresponding to TE polarized wave as shown in Fig. 7. The transmittance of 1-D photonic structures of period number $N=1, 2, 4, 6, 8, 10$ and 12 have been shown by solid green line, solid red line, solid

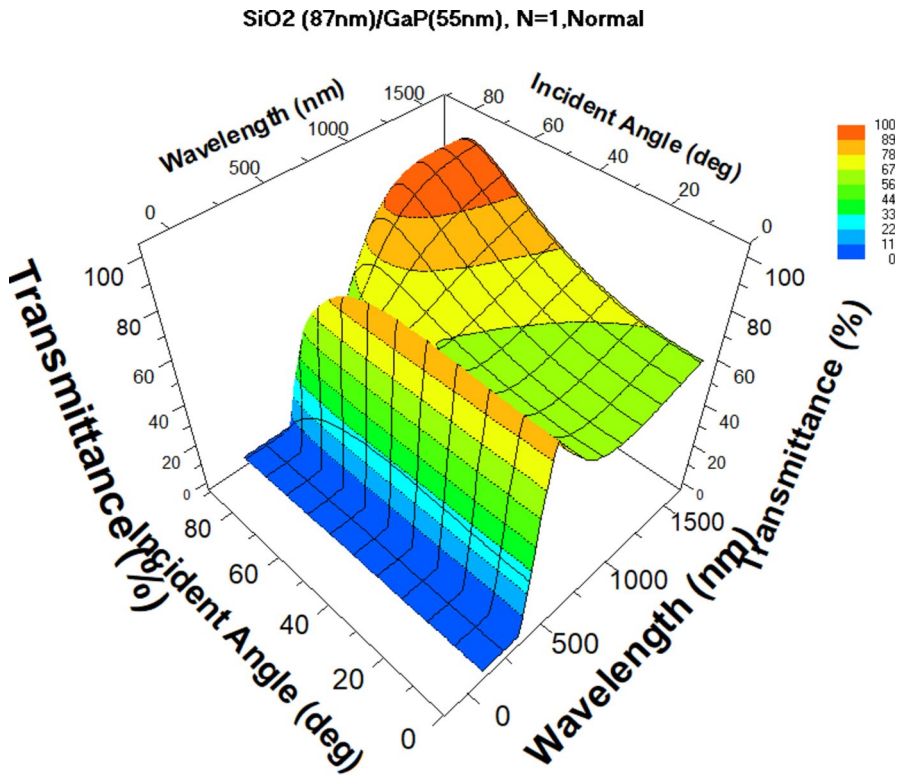


Fig. 5 An effect of incident angle on the wavelength dependent percentage transmittance of 1-D photonic structure composed of alternating material layers of SiO₂ and GaP of period number $N=1$

blue line, red dashed line, pink dashed line, blue dashed line and black dashed line respectively in Fig. 7. The transmittance of the 1-D photonic structure $N=1$ shown in green colour contains a single transmittance peak of almost unit transmittance at lower wavelength region. Further increase in N results the decrease in the transmittance which reaches to minimum and again start increasing with wavelength. The structure with $N=2$ results the increase in the number of transmission peaks but still no clear PBG is obtained in visible region. For higher values of period number from $N=4$ to $N=12$, the second PBG is formed. The widths of PBGs of structures of $N=4$ to $N=12$ are almost unchanged and become independent of number of unit cells (N). The number of transmission peaks towards infrared wavelength range also increases with the increase in N , which is similar to Ref. [41]. The reason behind the existence of increased transmission peaks is due to interference between the reflected light form the interfaces of the structure. The transmittance of PBG region reduces to zero for higher values of N along with sharp boundary edges as evident from Fig. 7. The scattering losses in the present calculations have been neglected. Authors have only focused on the reflectance phase, transmittance

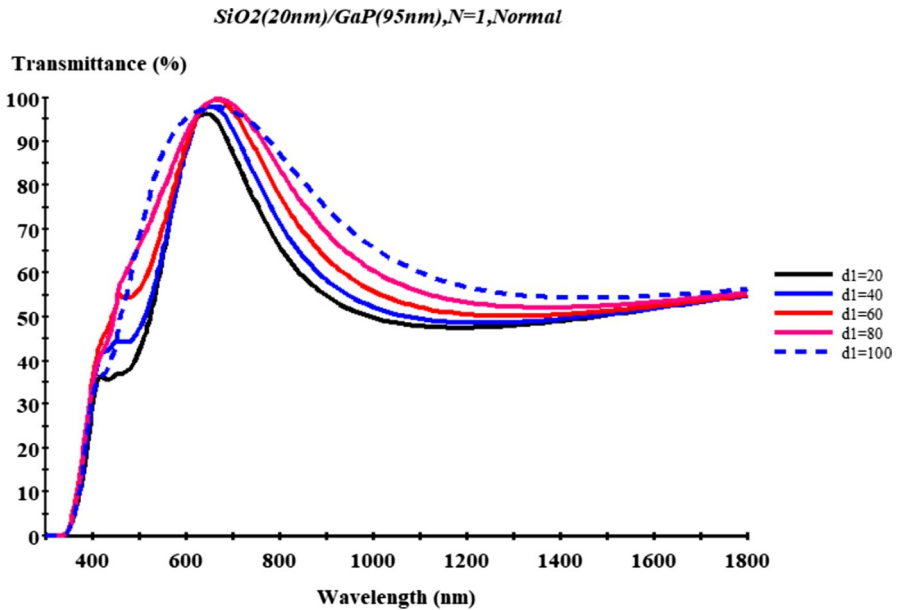


Fig. 6 Transmittance of the 1D photonic structures $(\text{SiO}_2/\text{GaP})^N$ with SiO_2 material layer thickness as $d_1=20$ nm, 40 nm, 60 nm, 80 nm and 100 nm whereas the thickness of GaP layer of all structures is fixed to $d_2=95$ nm, $N=1$ and $\theta=0^\circ$

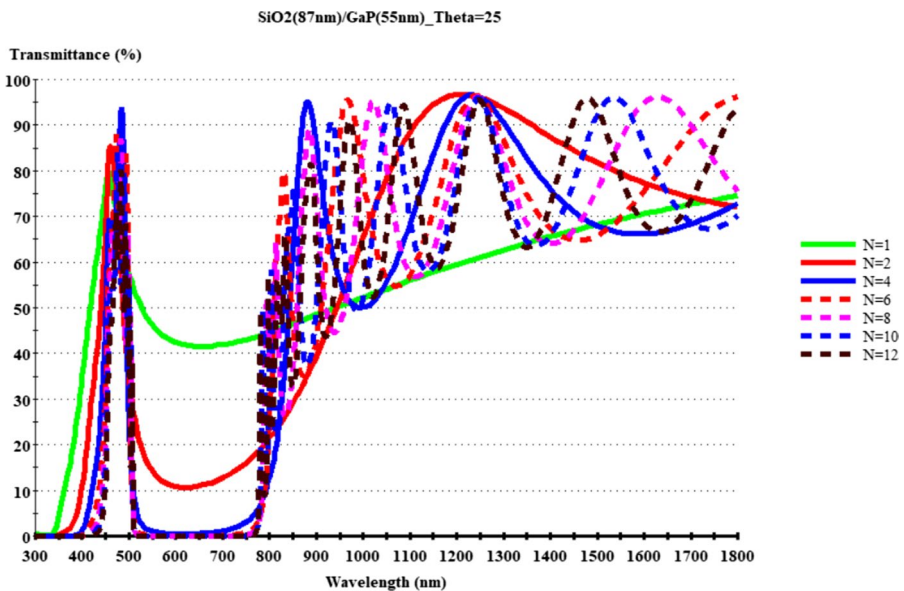


Fig. 7 Transmittance of 1-D photonic structures $(\text{SiO}_2/\text{GaP})^N$ of period number $N=1, 2, 4, 6, 8, 10$ and 12 shown by solid green line, solid red line, solid blue line, red dashed line, pink dashed line, blue dashed line and black dashed line respectively. The thickness of layers SiO_2 and GaP are $d_1=87$ nm and $d_2=55$ nm respectively at $\theta=25^\circ$ corresponding to TE wave only

and absorbance characteristics of the present work due to the weak scattering in the proposed structure. In future work scattering may also be considered.

4 Conclusion

In conclusion, we have demonstrated the feasibility of building a 1-D photonic structure composed of alternate layers of silicon dioxide and gallium phosphide materials. The optical characteristics of the proposed 1-D photonic structures $(\text{SiO}_2/\text{GaP})^N$ of different period number N have been studied by employing the transfer matrix technique. The utilization of GaP material in the design of the proposed structure is due to its exceptionally good performance in a variety of applications such as mid-IR frequency combs, ultra-broadband supercontinuum generation, waveguide sidewall roughness reduction and improvement in dispersion architecture. The 1-D photonic structures of this work can be used for design and development of the versatile photonic devices. Such structures may be very useful for regulating and enhancing the luminescence of nanostructures composed of GaP and/or SiO_2 materials due to large photonic band gaps.

Acknowledgements The current work was assisted financially to the Dean of Science and Research at King Khalid University via the Large Group Project under grant number RGP. 2/220/43

Author contributions A.H.A. conceived the designs. A.H.A., B.S., A.M., S.A.A., S.K.A, E.F., and M.F. designed and conducted the analyses. A.H.A., B.S., A.M., S.A.A., S.K.A, E.F., and d M.F. analyzed the results. All authors reviewed the manuscript.

Data availability and materials The datasets used and/or analyzed during the current study are available from the corresponding author on reasonable request.

Code availability No code is used in this study.

Declarations

Conflict of interest The authors declare no conflict of interest.

References

1. Joannopoulos, J. D., Johnson, S. G., Winn, J. N., & Meade, R. D. (2011) *Photonic crystals: Molding the flow of light* (2nd edn.). Princeton University Press. <https://press.princeton.edu/books/hardcover/9780691124568/photonic-crystals>. Accessed 31 January 2021
2. Kumar, N., & Suthar, B. (2019). *Advances in photonic crystals and devices first*. Boca Raton: CRC Press. <https://doi.org/10.1201/9781351029421>
3. Pandey, G. N., Suthar, B., Kumar, N., & Thapa, K. B. (2021). Omnidirectional reflectance of superconductor-dielectric photonic crystal in THz frequency range. *Journal of Superconductivity and Novel Magnetism*, 34, 2031–2039. <https://doi.org/10.1007/s10948-021-05962-3>
4. Chhipa, M. K., Madhav, B. T. P., Robinson, S., Janyani, V., & Suthar, B. (2021). Realization of all-optical logic gates using a single design of 2D photonic band gap structure by square ring resonator. *Optical Engineering*, 60, 075104. <https://doi.org/10.1117/1.oe.60.7.075104>
5. Biswas, U., Rakshit, J. K., Das, J., Bharti, G. K., Suthar, B., Amphawan, A., & Najjar, M. (2021). Design of an ultra-compact and highly-sensitive temperature sensor using photonic crystal based

- single micro-ring resonator and cascaded micro-ring resonator. *SILICON*, 13, 885–892. <https://doi.org/10.1007/s12633-020-00489-z>
6. Zaky, Z. A., & Aly, A. H. (2020). Theoretical study of a tunable low-temperature photonic crystal sensor using dielectric-superconductor nanocomposite layers. *Journal of Superconductivity and Novel Magnetism*, 33, 2983–2990. <https://doi.org/10.1007/s10948-020-05584-1>
 7. Ankita, Bissa, S., Suthar, B., & Bhargava, A. (2022). Graded photonic crystal as improved sensor for nanobiophotonic application. *Macromolecular Symposium*, 401, 2100319. <https://doi.org/10.1002/masy.202100319>
 8. Suthar, B., Kumar, N., & Taya, S. A. (2022). Design and analysis of tunable multichannel transmission filters with a binary photonic crystal of silver/silicon. *The European Physical Journal Plus*, 137(12), 1–6. <https://doi.org/10.1140/EPJP/S13360-022-03533-6>
 9. Kumar, N., Sonika, Suthar, B., & Rostami, A. (2023). Novel optical behaviors of metamaterial and polymer-based ternary photonic crystal with lossless and lossy features. *Optics Communications*, 529, 129073. <https://doi.org/10.1016/J.OPTCOM.2022.129073>
 10. Aly, A. H., & Elsayed, H. A. (2019). Transmittance properties of one-dimensional metallic-dielectric photonic crystals in near-zero permittivity. *Physica Scripta*, 94, 125501. <https://doi.org/10.1088/1402-4896/ab2b7b>
 11. Awad, M. A., & Aly, A. H. (2019). Experimental and theoretical studies of hybrid multifunctional TiO₂/TiN/TiO₂. *Ceramics International*, 45, 19036–19043. <https://doi.org/10.1016/J.CERAMINT.2019.06.145>
 12. Amiri, I. S., Paul, B. K., Ahmed, K., Aly, A. H., Zakaria, R., Yupapin, P., & Vigneswaran, D. (2019). Tri-core photonic crystal fiber based refractive index dual sensor for salinity and temperature detection. *Microwave and Optical Technology Letters*, 61, 847–852. <https://doi.org/10.1002/MOP.31612>
 13. Kumar, A., Suthar, B., Kumar, V., Singh, K. S., & Bhargava, A. (2012). Tunable wavelength demultiplexer for DWDM application using 1-D photonic crystal. *Progress in Electromagnetics Research Letters*, 33, 27–35. <https://doi.org/10.2528/PIERL12042009>
 14. Mohebzadeh-Bahabady, A., & Olyae, S. (2019). Designing low power and high contrast ratio all-optical NOT logic gate for using in optical integrated circuits. *Optical and Quantum Electronics*, 51, 1–13. <https://doi.org/10.1007/s11082-018-1715-6>
 15. Kumar, A., Kumar, V., Suthar, B., Ojha, M., Singh, K. S., & Ojha, S. P. (2013). Trapping of light in nonlinear 1-D photonic crystal. *IEEE Photonics Technology Letters*, 25, 279–282. <https://doi.org/10.1109/LPT.2012.2235140>
 16. Ankita, Bissa, S., Suthar, B., Nayak, C., & Bhargava, A. (2022). An improved optical biosensor design using defect/metal multilayer photonic crystal for malaria diagnosis. *Results in Optics*, 9, 100304. <https://doi.org/10.1016/j.rio.2022.100304>
 17. Aly, A. H., Mohamed, D., Zaky, Z. A., Matar, Z. S., Abd El-Gawaad, N. S., Shalaby, A. S., Tayeboun, F., & Mohaseb, M. (2021). Novel biosensor detection of tuberculosis based on photonic band gap materials. *Materials Research*, 24, 20200483. <https://doi.org/10.1590/1980-5373-MR-2020-0483>
 18. Rafiee, E. (2023). Photonic crystal based biosensor for diagnosis of kidney failure and diabetes. *Plasmonics*. <https://doi.org/10.1007/s11468-023-02014-5>
 19. Rafiee, E., Emami, F., & Negahdari, R. (2018). Design of a novel nano plasmonic-dielectric photonic crystal power splitter suitable for photonic integrated circuits. *Optik*, 172, 234–240. <https://doi.org/10.1016/j.ijleo.2018.06.006>
 20. Rafiee, E., & Emami, F. (2017). Design of a novel all-optical ring shaped demultiplexer based on two-dimensional photonic crystals. *Optik*, 140, 873–877. <https://doi.org/10.1016/j.ijleo.2017.05.010>
 21. Rafiee, E., & Emami, F. (2018). Realization of tunable optical channel drop filter based on photonic crystal octagonal shaped structure. *Optik*, 171, 798–802. <https://doi.org/10.1016/j.ijleo.2018.06.146>
 22. Wilson, D. J., Schneider, K., Hönl, S., Anderson, M., Baumgartner, Y., Czornomaz, L., Kippenberg, T. J., & Seidler, P. (2020). Integrated gallium phosphide nonlinear photonics. *Nature Photonics*, 14, 57–62. <https://doi.org/10.1038/s41566-019-0537-9>
 23. Haynes, W. M. (2016). *CRC handbook chemistry and physics*. Boca Raton: CRC Press.
 24. Rivoire, K., Kinkhabwala, A., Hatami, F., Masselink, W. T., Avlasevich, Y., Müllen, K., Moerner, W. E., & Vučković, J. (2009). Lithographic positioning of fluorescent molecules on high-Q photonic crystal cavities. *Applied Physics Letters*, 95, 123113. <https://doi.org/10.1063/1.3232233>
 25. Li, L., Schröder, T., Chen, E. H., Bakhru, H., & Englund, D. (2015). One-dimensional photonic crystal cavities in single-crystal diamond. *Photonics and Nanostructures-Fundamentals and Applications*, 15, 130–135. <https://doi.org/10.1016/j.photonics.2015.03.002>

26. Gan, X., Pervez, N., Kymissis, I., Hatami, F., & Englund, D. (2012). A high-resolution spectrometer based on a compact planar two dimensional photonic crystal cavity array. *Applied Physics Letters*, *100*, 231104. <https://doi.org/10.1063/1.4724177>
27. Rivoire, K., Lin, Z., Hatami, F., Masselink, W. T., & Vučković, J. (2009). Second harmonic generation in gallium phosphide photonic crystal nanocavities with ultralow continuous wave pump power. *Optics Express*, *17*, 22609–22615.
28. Shambat, G., Rivoire, K., Lu, J., Hatami, F., & Vučković, J. (2010). Tunable-wavelength second harmonic generation from GaP photonic crystal cavities coupled to fiber tapers. *Optics Express*, *18*, 12176–12184. <https://doi.org/10.1364/oe.18.012176>
29. Rivoire, K., Lin, Z., Hatami, F., & Vučković, J. (2010). Sum-frequency generation in doubly resonant GaP photonic crystal nanocavities. *Applied Physics Letters*, *97*, 043103. <https://doi.org/10.1063/1.3469936>
30. Choy, M. M., & Byer, R. L. (1976). Accurate second-order susceptibility measurements of visible and infrared nonlinear crystals. *Physical Review B*, *14*, 1693. <https://doi.org/10.1103/PhysRevB.14.1693>
31. Bond, W. L. (1965). Measurement of the refractive indices of several crystals. *Journal of Applied Physics*, *36*, 1674–1677. <https://doi.org/10.1063/1.1703106>
32. Palik, E. D. (2012). *Handbook of optical constants of solids*. <https://doi.org/10.1016/C2009-0-20920-2>
33. Suthar, B., & Bhargava, A. (2012). Enlargement of omni-directional reflection by cascading chalcogenide based photonic crystals. *Optics Communication*, *285*, 1481–1485. <https://doi.org/10.1016/j.optcom.2011.10.033>
34. Aly, A. H., Elsayed, H. A., & Hamdy, H. S. (2010). The optical transmission characteristics in metallic photonic crystals. *Materials Chemistry and Physics*, *124*(1), 856–860. <https://doi.org/10.1016/j.matchemphys.2010.08.006>
35. Liu, Y., Yi, L., Hu, X. G., Duan, Y. F., & Yang, Z. Z. (2015). Phase retarder based on one-dimensional photonic crystals composed of plasma and mu-negative materials. *Physics of Plasmas*, *22*, 012101. <https://doi.org/10.1063/1.4905514>
36. Kumar, N., & Ojha, S. P. (2013). Toward modal dispersion characteristics of a new unconventional optical waveguide with a core cross-section of plano-concave lens shape. *Optik*, *124*(9), 773–777. <https://doi.org/10.1016/j.ijleo.2012.01.009>
37. Kumar, N., & Ojha, S. (2008). Photonic crystals as infrared broadband reflectors with different angles of incidence: a comparative study. *Progress in Electromagnetics Research*, *80*, 431–445. <https://doi.org/10.2528/PIER07120502>
38. Centini, M., Sibilia, C., Scalora, M., D'Aguzzo, G., Bertolotti, M., Bloemer, M. J., Bowden, C. M., & Nefedov, I. (1999). Dispersive properties of finite, one-dimensional photonic band gap structures: Applications to nonlinear quadratic interactions. *Physical Review E - Covering Statistical, Nonlinear, Biological, and Soft Matter Physics*, *60*, 4891. <https://doi.org/10.1103/PhysRevE.60.4891>
39. Sayed, H., Al-Dossari, M., Ismail, M. A., Abd El-gawaad, N. S., & Aly, A. H. (2022). Theoretical analysis of optical properties for amorphous silicon solar cells with adding anti-reflective coating photonic crystals. *Photonics*, *9*, 813. <https://doi.org/10.3390/photonics9110813>
40. Kumari, N., Varshney, A. D., Awasthi, S. K., Shiveshwari, L., & Aly, A. H. (2022). Tunable photonic bandgap and reflection phase shift properties of 1D binary photonic crystal consisting of double negative and magnetic cold plasma materials. *Physics of Plasmas*, *29*, 042110. <https://doi.org/10.1063/5.0071898>
41. Alamrani, F., & Alsharaeh, E. (2022). Controlling the bandgaps of one-dimensional TiO₂/SiO₂, TiO₂/SnO₂, and SiO₂/SnO₂ photonic crystals using the transfer matrix method. *Optics and Photonics Journal*, *12*, 171–189. <https://doi.org/10.4236/opj.2022.127013>

Publisher's Note Springer Nature remains neutral with regard to jurisdictional claims in published maps and institutional affiliations.

Springer Nature or its licensor (e.g. a society or other partner) holds exclusive rights to this article under a publishing agreement with the author(s) or other rightsholder(s); author self-archiving of the accepted manuscript version of this article is solely governed by the terms of such publishing agreement and applicable law.

Authors and Affiliations

**Arafa H. Aly¹ · Bhuvneshwer Suthar^{2,3} · Azath Mubarakali^{1,3} ·
Suhad Ali Osman Abdallah⁴ · S. K. Awasthi⁵ · Emadelden Fouad⁶ · M. I. Fathy¹**

✉ Arafa H. Aly
arafa.hussien@science.bsu.edu.eg; arafaaly@aucegypt.edu

¹ TH-PPM Group, Physics Department, Faculty of Sciences, Beni-Suef University,
Beni Suef 62514, Egypt

² Nanophysics Laboratory, Department of Physics, Government Dungar College, Bikaner,
Rajasthan 334001, India

³ College of Computer Science, King Khalid University, Abha, Saudi Arabia

⁴ Department of Mathematics, Faculty of Science, King Khalid University, Abha 62529,
Saudi Arabia

⁵ Department of Physics and Material Science and Engineering, Jaypee Institute of Information
Technology, Noida 201304, India

⁶ Department of Engineering Physics, Florida Polytechnic University, Lakeland, USA